Journal of Japan Association for Earthquake Engineering, Vol. 25, No. 8, 2025

SHAKING TABLE TEST AND FINITE ELEMENT ANALYSIS FOR BASE-INSULATED BUILDING MODEL WITH DISPLACEMENT CONTROL MATERIAL AND MAGNETS (CONSIDERING MAGNETIZATION AND EDDY CURRENT IN INSULATING LAYER)

Takaharu NAKANO[1], Hisatoshi KASHIWA[2] and Yuji MIYAMOTO[3]

[1] Member, Dr. Eng., Associate Professor, Multidisciplinary Resilience Research Center, Institute of Science Tokyo, Kanagawa, Japan, nakano.t.0672@m.isct.ac.jp
[2] Member, Dr. Eng., Professor, Graduate School of Engineering, The University of Osaka, Osaka, Japan, kashiwa@arch.eng.osaka-u.ac.jp
[3] Member, Dr. Eng., Professor, Fukui University of Technology, Fukui, Japan/ Emeritus Professor, The University of Osaka, Osaka, Japan, miyamoto@fukui-ut.ac.jp

ABSTRACT: To reduce the seismic response of small buildings, the authors propose a magnetically levitated foundation insulated from the ground by magnets and supported by a displacement control material. In this study, metal components were used to improve the levitation force and damping characteristics. A static loading test indicated that steel plates on the magnets increased the levitation force. Electromagnetic field analysis showed that a copper plate between the magnets acted as an eddy-current damper and could be represented by a Maxwell material. In addition, the seismic response of a magnetically levitated foundation was discussed based on a shaking table test and structural analysis.

Keywords: *Magnetic levitation, Seismic response reduction, Magnetic material, Eddy-current damper*

1. INTRODUCTION

Learning from the damage to buildings caused by the 1995 Hyogo-ken Nanbu earthquake, seismic isolation technology was developed as the primary method for reducing the seismic response of buildings. The effectiveness of seismic isolation in structures has been confirmed to a certain extent by several subsequent earthquakes. However, seismic isolated structures require clearance around them, and there is a debate regarding their ultimate behavior, including the risk of collision of the seismic isolation layer with the retaining wall owing to excessive deformation. Therefore, the development of new response-reduction technologies is beneficial.

The seismic motion that reaches a building site from the epicenter of an earthquake is input to the building via the boundary between the ground and foundation. If the bottom of the foundation is

insulated from the ground and the transmission path of the seismic motion is cut off, the seismic response of the building could be significantly reduced. Magnetic levitation[1), 2)], as well as air levitation[3), 4)], are some of the most promising methods to achieve this goal. However, Earnshaw's theorem[5)] states that stable levitation cannot be achieved using only the magnetic force generated by a classical static magnetic field. To escape the yoke of this theorem, the structures are levitated in Ref. 1) by changing the magnetic field through control of the current applied to the electromagnets and in Ref. 2) by using the restoring force caused by the quantum mechanical phenomena of superconductors.

Miyamoto et al.[6), 7)] proposed a magnetically levitated earthquake-insulated foundation named "Zesshin," which is insulated from the ground by permanent magnets at the bottom and supported by displacement control materials at the sides, and conducted a model shaking table experiment. The structure of this mechanism is illustrated in Fig. 1. The purpose of this mechanism is to reduce the earthquake response of small buildings. In the experiments described in Ref. 6), a building model with a mass of approximately 2 kg was used, and a cement-based compound geomaterial mixed with fibers was employed as the displacement control material. In the experiments described in Ref. 7), the mass of the building model increased to approximately 14 kg, and a soft and high-ductility polymer was used as the displacement control material. The results of both experiments showed that the displacement control material stabilized the magnetically levitated foundation and the building response reduced owing to magnetic levitation. The authors[8)] calculated the force between the magnets for the experimental model in Ref. 7), and discussed properties such as nonlinearity and negative stiffness. Negative stiffness hinders stable magnetic levitation; therefore, the key objective of the magnetically levitated foundation in this study was to neutralize this by using displacement control materials[8)]. Other roles of the displacement control material are the elimination of clearance and use of its inherent energy-absorption ability[9)].

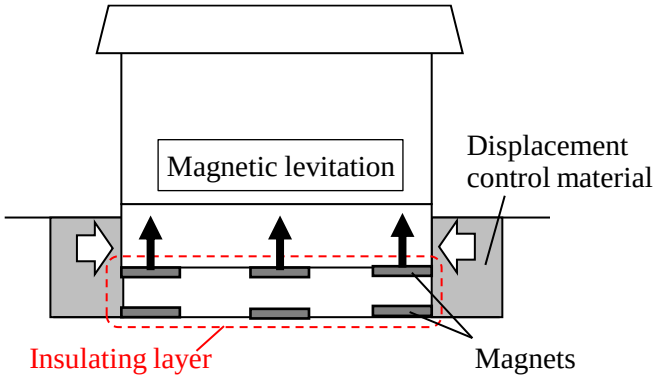

Fig. 1 Schematic of magnetically levitated foundation

In the experiments described in Refs. 6) and 7), to simplify the electromagnetic problems, nothing was inserted into the gap between the magnets, and magnetic materials such as iron were excluded from the vicinity of the magnets. Therefore, the formula for calculating the magnetic force was based solely on Coulomb's law[8)]. However, when magnets are used alone, much of the magnetic flux emitted from the magnetic poles leaks into space; therefore, in this study, we attempted to utilize such a magnetic flux. As shown in Fig. 2, a magnetic material (steel plate) and conductor (copper plate) were used in combination with magnets to increase the levitation force and damping of the foundation, respectively. In Fig. 2(a), a steel plate is magnetized by the magnets placed at the bottom of the foundation. The steel plate repels the magnets on the ground, allowing the foundation to be levitated more efficiently with the same size of magnets. As shown in Fig. 2(b), eddy currents are generated in a copper plate owing to the relative motion between the foundation and ground, generating a damping force that converts the kinetic energy of the building into electricity and dissipates it as heat. Therefore, with the simple change of attaching a steel or copper plate, the electromagnetic phenomena becomes more complex than those in Ref. 8). Therefore, in Sections 2 and 3, we first discuss the characteristics of the insulating layers shown in Fig. 2. Section 4 examines the seismic response of a building model in which magnetically levitated foundations were coupled with displacement control materials and superstructures.

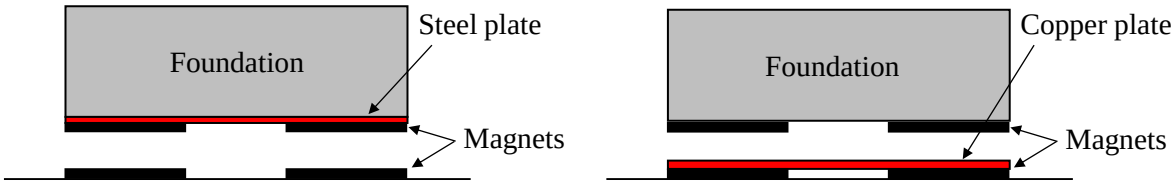

(a) A magnetic material (steel plate) is used:
The steel plate is magnetized by a magnet under the foundation, causing it to repel the magnet on the ground.

(b) A conductor (copper plate) is used:
The relative motion between the foundation and the ground generates eddy currents in the copper plate, providing a damping force.

Fig. 2 Insulating layer of magnetically levitated foundation using magnetic material or conductor

2. LEVITATION FORCE ACTING ON MAGNETICALLY LEVITATED FOUNDATION USING MAGNETIC MATERIAL

2.1 Formulation based on the theory of static magnetic fields

The magnetic intensity of magnetic materials, such as a magnet or a steel plate, is expressed in magnetization $\boldsymbol{J}$ (unit: T). Generally, the magnetization of magnetic materials depends on the magnetic field. In the system shown in Fig. 2(a), the magnetic field generated by the magnets at the bottom of the foundation magnetizes the steel plate above them, and the magnetic force acting between the steel plate and magnets on the ground is used to levitate the foundation more efficiently.

2.1.1 Magnetic force acting on a magnetic material

When calculating the magnetic force, it is convenient to replace the magnetic material with the magnetic charge (Wb). The volume density of magnetic charge equivalent to a magnetic material is $-\mathrm{div}\boldsymbol{J}$, and the surface density is $\boldsymbol{J}\cdot\boldsymbol{n}$ ($\boldsymbol{n}$: outward unit normal vector on the surface)[10)–12)]. Therefore, the magnetic force $\boldsymbol{F}$ acting on a uniformly magnetized cuboid M_1 is given by Eq. (1) using the intensity of the magnetic field $\boldsymbol{H}$ (A/m).

$$\boldsymbol{F} = \oiint_S \boldsymbol{H}(\boldsymbol{r})(\boldsymbol{J}\cdot\boldsymbol{n})\mathrm{d}S \tag{1}$$

where S is the surface of cuboid M_1, and $\boldsymbol{r}$ is the field point (the point where the infinitesimal surface dS is located).

The magnetic field used in Eq. (1) does not need to include the components caused by the cuboid M_1 if it is a static magnetic field problem[13)]. The magnetic field $\boldsymbol{H}$ caused by another uniformly magnetized cuboid M_2 is given by Eq. (2), which is an extension of the formula in Ref. 8).

$$\boldsymbol{H}(\boldsymbol{r}) = \oiint_{S'} \frac{(\boldsymbol{J}\cdot\boldsymbol{n})\mathrm{d}S'}{4\pi\mu_0}\frac{\boldsymbol{r}-\boldsymbol{r}'}{|\boldsymbol{r}-\boldsymbol{r}'|^3} = \frac{1}{4\pi\mu_0}\sum_{\alpha=1}^{2}\sum_{\beta=1}^{2}\sum_{\gamma=1}^{2}(-1)^{\alpha+\beta+\gamma}\boldsymbol{M}\left(\boldsymbol{r}-\boldsymbol{r}'_{\alpha\beta\gamma}\right)\begin{Bmatrix}J_x\\J_y\\J_z\end{Bmatrix} \tag{2}$$

$$\boldsymbol{M}(\boldsymbol{R}) = \begin{bmatrix} \tan^{-1}\dfrac{YZ}{X|\boldsymbol{R}|} & -\tanh^{-1}\dfrac{Z}{|\boldsymbol{R}|} & -\tanh^{-1}\dfrac{Y}{|\boldsymbol{R}|} \\ -\tanh^{-1}\dfrac{Z}{|\boldsymbol{R}|} & \tan^{-1}\dfrac{ZX}{Y|\boldsymbol{R}|} & -\tanh^{-1}\dfrac{X}{|\boldsymbol{R}|} \\ -\tanh^{-1}\dfrac{Y}{|\boldsymbol{R}|} & -\tanh^{-1}\dfrac{X}{|\boldsymbol{R}|} & \tan^{-1}\dfrac{XY}{Z|\boldsymbol{R}|} \end{bmatrix} \tag{3}$$

where μ_0 is the permeability of a vacuum, S' is the surface of cuboid M_2, $\boldsymbol{r}'$ is the source point (the point where the infinitesimal surface dS' is located), $\boldsymbol{r}'_{\alpha\beta\gamma} = \{x_\alpha, y_\beta, z_\gamma\}^T$ denotes the vertices of the cuboid M_2 (the subscripts are 1 or 2), $\boldsymbol{J} = \{J_x, J_y, J_z\}^T$, and $\boldsymbol{R} = \{X, Y, Z\}^T$. The superscript T represents transpose. Further, let $x_1 < x_2$, $y_1 < y_2$, and $z_1 < z_2$.

The diagonal components of the matrix $\boldsymbol{M}$ may be indefinite at points $\boldsymbol{r}$ on the same plane as the faces of the cuboid. In addition, the non-diagonal components may be indefinite at points $\boldsymbol{r}$ on the lines containing the edges. If these issues become a problem when calculating the external magnetic field, the magnetic field can converge to a finite value by calculating the limit of the sum, rather than calculating the limit for each term in Eq. (2).

2.1.2 How to calculate magnetization

The value of $\boldsymbol{J}$ used in Eqs. (1) and (2) is constant for magnets. However, for steel plates, it is calculated using the method in Ref. 14) based on the magnetic constitutive law. The magnetic constitutive law is expressed by Eq. (4) using the magnetic flux density $\boldsymbol{B}$ (T).

$$\boldsymbol{B}(\boldsymbol{r}) = \mu_0 \boldsymbol{H}(\boldsymbol{r}) + \boldsymbol{J}(\boldsymbol{r}) \tag{4}$$

In the linear magnetic constitutive law, $\boldsymbol{B} = \mu\boldsymbol{H}$ (μ: permeability), $\boldsymbol{H}$ can be eliminated from Eq. (4) to obtain Eq. (5)[14].

$$\boldsymbol{J}(\boldsymbol{r}) = (1 - \mu_0/\mu)\boldsymbol{B}(\boldsymbol{r}) \tag{5}$$

The steel plate is divided into N uniformly magnetized cuboids[14], and it is assumed that the magnetization $\boldsymbol{J}_k$ of the kth cuboid is determined by the magnetic flux density $\boldsymbol{B}(\boldsymbol{r}_k)$ at the center $\boldsymbol{r}_k$. The magnetic flux density is caused by both the steel plate and magnets. In the original reference[14], the magnetic material was replaced with an equivalent current and the magnetic flux density was calculated using the Biot–Savart law. When using an equivalent magnetic charge, it is possible to calculate the intensity of the magnetic field $\boldsymbol{H}(\boldsymbol{r}_k)$ generated at point $\boldsymbol{r}_k$ by a steel plate and magnets using Eq. (2), and then convert the result into the magnetic flux density $\boldsymbol{B}(\boldsymbol{r}_k)$ using Eq. (4). Considering Eq. (5) at points $\boldsymbol{r}_1$ to $\boldsymbol{r}_N$, we obtain simultaneous linear equations for magnetizations $\boldsymbol{J}_1$ to $\boldsymbol{J}_N$.

2.2 Levitation force test

The levitation force–gap relationship of a magnetically levitated foundation using a steel plate was measured using a levitation force test to investigate the effect of the magnetic material on the levitation force and confirm the validity of the theoretical solution obtained by the above method.

The loading conditions are shown in Fig. 3. The specimen consisted of an aluminum foundation (200 mm × 200 mm × 65 mm), an SS400 steel plate (200 mm × 200 mm × 3.2 mm), and magnets (70 mm × 70 mm × 5 mm). The magnets were attached to the four corners at the bottom of the foundation to sandwich the steel plate. The magnets were neodymium magnets magnetized in the thickness direction with a residual magnetic flux density of 1.2 T. The same type of magnet was attached to the ground, which repelled the magnet at the bottom of the foundation. The foundation and steel plate were bonded with a nonmagnetic adhesive, and the steel plate and magnets were attracted by a magnetic force. An aluminum channel-shaped guide was attached to the side of the foundation to prevent horizontal displacement, and it slid vertically to create a roller condition. In the test, weights were individually placed on the foundation to obtain the relationship between the gap between the magnets and the levitation force.

In the calculation based on the theory described in Section 2.1, the magnetization was set to the same value as the residual magnetic flux density, and the steel plate was divided into 40 × 40 × 1 cuboid elements. According to references[15, 16], the relative permeability μ/μ_0 of the SS400 material is approximately 150 to 2000 when unloaded. Because the sensitivity of μ/μ_0 in this range to the levitation force of this test specimen is low, this study assumed $\mu/\mu_0 = 1000$.

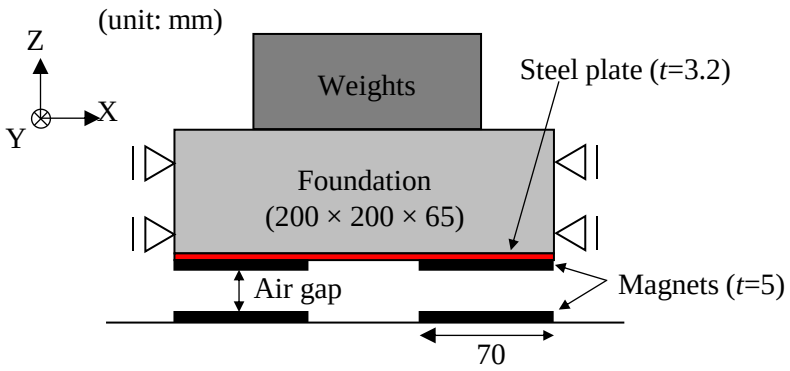

Fig. 3 Cross-section of specimen for levitation force test

Figure 4 shows a comparison of the experimental and calculated values of the levitation force–gap relationship. When a steel plate was used, the levitation force on the foundation for the same gap was larger. In addition, the calculated values agreed with the experimental values regardless of whether the steel plate was present. Therefore, the levitation force of the foundation can be calculated even if the foundation contains a magnetic material whose magnetization is not constant.

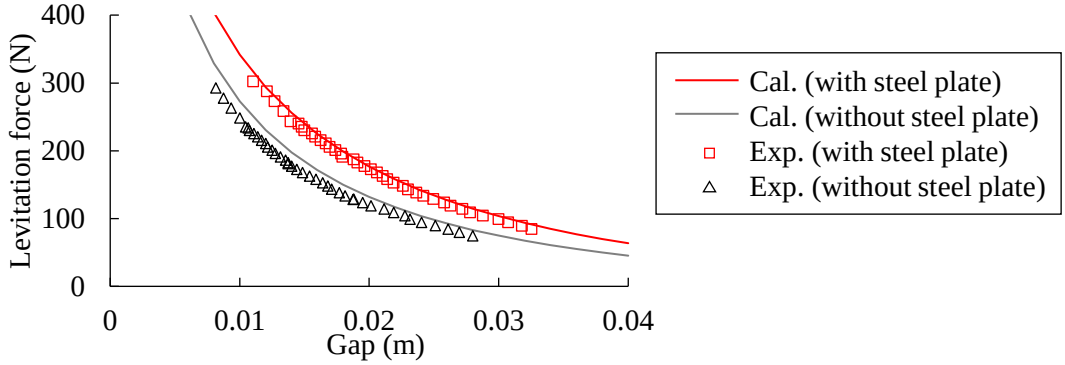

Fig. 4 Levitation force vs. gap relationship

Figure 5 shows the magnetization distribution of the steel plate when the gap between the magnets is 25 mm. While the magnets are magnetized uniformly in the vertical direction, the magnetization of the steel plate has a predominantly horizontal component, with its peak values appearing above the edge of the magnets. This is because the external magnetic field of the magnets is non-uniform, as shown in Fig. 6, and forms a vortex-shaped magnetic field near the edge of the magnets, causing the steel plate inserted there to be magnetized in the tangential direction.

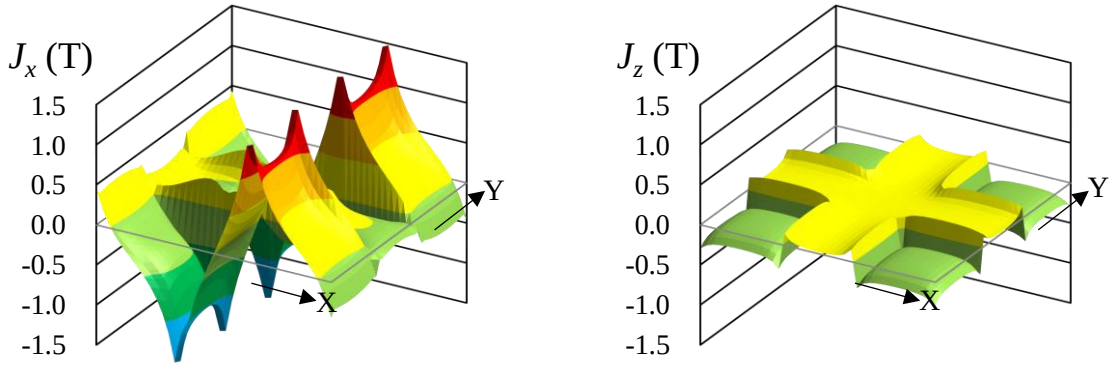

(a) X component (b) Z component

Fig. 5 Magnetization distribution of steel plate

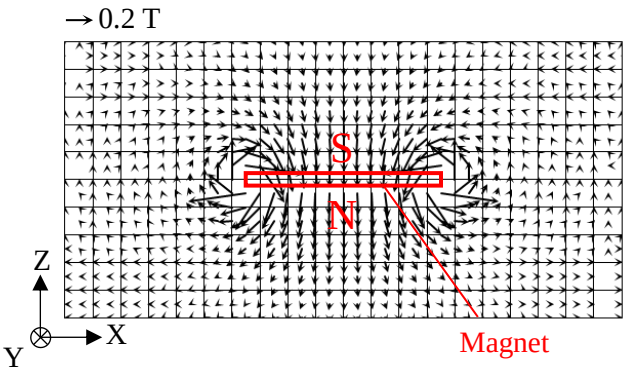

Fig. 6 External magnetic field of a magnet

3. DAMPING CHARACTERISTICS OF MAGNETICALLY LEVITATED FOUNDATION USING CONDUCTOR

3.1 Formulation based on electromagnetic induction theory

When a relative velocity occurs between the magnetically levitated foundation and ground, the magnetic field between the magnets changes over time. Therefore, if a conductor is inserted as shown in Fig. 2(b), eddy currents are generated according to the law of electromagnetic induction. The electromagnetic force caused by the magnetic field of the magnet acts on the eddy currents, and the reaction force is transmitted to the magnet. From the perspective of energy, the kinetic energy of the building is converted into electricity, which is then converted into heat and discarded owing to the electrical resistance of the conductor. In other words, the conductor functions as an eddy current damper.

Eddy currents have the function of self-induction, which prevents their own changes, and it is expected that the phase of the eddy current lags behind that of the relative velocity. A viscoelastic model combining a spring and dashpot was proposed as the mechanical model of an eddy current damper that considers the effects of self-induction[17), 18)].

In this section, we theoretically examine the properties of an eddy current damper, with the aim of expressing it using a viscoelastic model. Here, we consider the eddy current to be a quasi-steady current[19)], and describe the phenomenon from the perspective of an observer who views the conductor as stationary.

3.1.1 For a single closed circuit

First, to obtain a rough understanding of the phenomenon, consider the simple problem shown in Fig. 7(a), in which a single closed circuit C exists near a vibrating magnet. However, the shape of the closed circuit and the distribution of the magnetic field are not specified.

When only the induced current I flows through the closed circuit C, the damping force F_x in the x-direction acting on the magnet is given by Eq. (6).

$$F_x = -\boldsymbol{e}_x \cdot \oint_C I \mathrm{d}\boldsymbol{s} \times \boldsymbol{B}_m = -I \iint_S \frac{\partial \boldsymbol{B}_m}{\partial x} \cdot \boldsymbol{n} \mathrm{d}S \equiv -\alpha_x I \tag{6}$$

where $\boldsymbol{e}_x$ is the unit vector in the x direction, d$\boldsymbol{s}$ is the infinitesimal vector along the circuit, S is the surface area enclosed by the closed circuit C, $\boldsymbol{n}$ is the unit normal vector on the infinitesimal surface dS, and $\boldsymbol{B}_m$ is the magnetic flux density of the magnet. In the second equality, we used the formulas for vector analysis, starting with the Stokes' theorem and Gauss's law for magnetic fields[20)].

The induced electromotive force V that drives the induced current follows Ohm's law in Eq. (7) and the law of electromagnetic induction in Eq. (8).

$$V = RI \tag{7}$$

$$V = -\frac{\mathrm{d}\Phi_m}{\mathrm{d}t} - \frac{\mathrm{d}\Phi_c}{\mathrm{d}t} \tag{8}$$

where R is the electrical resistance of the closed circuit C, Φ_m and Φ_c are the magnetic flux that penetrates the closed circuit C generated by the magnet and the induced current, respectively.

When the magnet moves in the x direction at a velocity v, the distribution of the magnetic flux density $\boldsymbol{B}_m$ moves in parallel by $v\Delta t$ in an infinitesimal time Δt. Therefore, the magnetic flux density at a fixed point changes by $-(\partial \boldsymbol{B}_m/\partial x)v\Delta t$, and $\mathrm{d}\Phi_m/\mathrm{d}t$ is given by Eq. (9).

$$\frac{\mathrm{d}\Phi_m}{\mathrm{d}t} = \frac{\mathrm{d}}{\mathrm{d}t}\iint_S \boldsymbol{B}_m \cdot \boldsymbol{n}\mathrm{d}S = -v\iint_S \frac{\partial \boldsymbol{B}_m}{\partial x} \cdot \boldsymbol{n}\mathrm{d}S = -\alpha_x v \tag{9}$$

Note that the coefficient α_x in Eqs. (6) and (9) is the same.

In addition, if the self-induction coefficient of the closed circuit C is L, then $\Phi_c = LI$, and Eq. (10) can be derived from Eqs. (7)–(9).

$$L\frac{\mathrm{d}I}{\mathrm{d}t} + RI = \alpha_x v \tag{10}$$

At a vibration $v = v_0 e^{j\omega t}$ that is sufficiently small to consider the coefficient α_x as a constant, Eq. (10) is equivalent to the AC circuit shown in Fig. 7(b), where the power source, coil, and resistor are connected in series. In this case, the steady-state response solution to Eq. (10) is expressed by Eq. (11).

$$I = \frac{\alpha_x v_0}{R + j\omega L} e^{j\omega t} = \frac{\alpha_x v_0}{R} \frac{1}{\sqrt{1 + (\omega\tau)^2}} e^{j(\omega t + \phi)} \tag{11}$$

$$\tau = L/R \tag{12}$$

$$\phi = -\tan^{-1}\omega\tau \tag{13}$$

where j is the imaginary unit, ω is the circular frequency of the magnet's vibration, and v_0 is the velocity amplitude of the magnet's vibration.

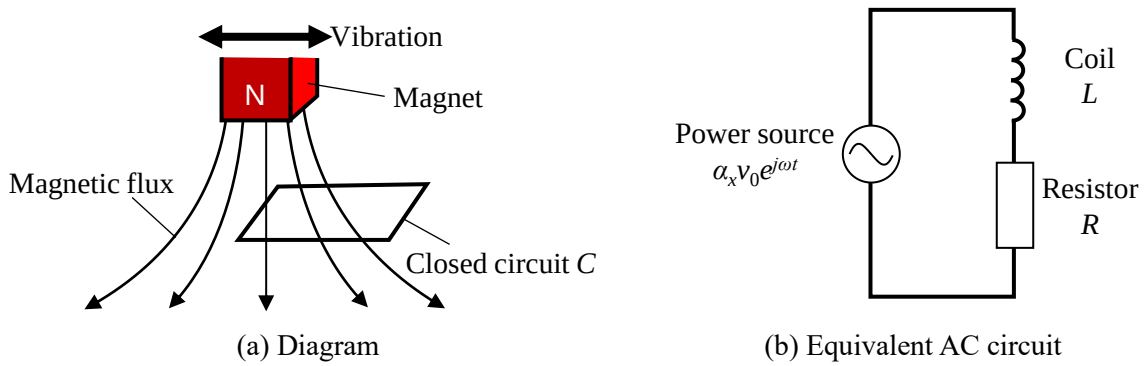

(a) Diagram (b) Equivalent AC circuit

Fig. 7 System consisting of a vibrating magnet and closed circuit

The energy ΔW that the damping force $F_x = -\alpha_x I$ takes from the building during one cycle is given by Eq. (14).

$$\Delta W = -\int_0^{2\pi/\omega} \mathrm{Re}(-\alpha_x I)\mathrm{Re}(v)\mathrm{d}t = \Delta W_0 \frac{2\omega\tau}{1+(\omega\tau)^2} \tag{14}$$

$$\Delta W_0 = \frac{\pi\alpha_x^2 x_0^2}{2L} = \frac{\pi(\Delta\Phi_m)^2}{2L} \tag{15}$$

where x_0 is the displacement amplitude of the magnet's vibration ($v_0 = \omega x_0$), and $\Delta\Phi_m$ is the amplitude of change of Φ_m. In addition, Re( ) represents the real part.

Figure 8 shows the graph of Eq. (14). ΔW is almost proportional to ω if $\omega\tau \ll 1$, and becomes nonlinear under the effect of self-induction as ω increases, reaching a maximum value of ΔW_0 at $\omega\tau = 1$. ΔW_0 depends on the shape of the closed circuit and the distribution of the magnetic field.

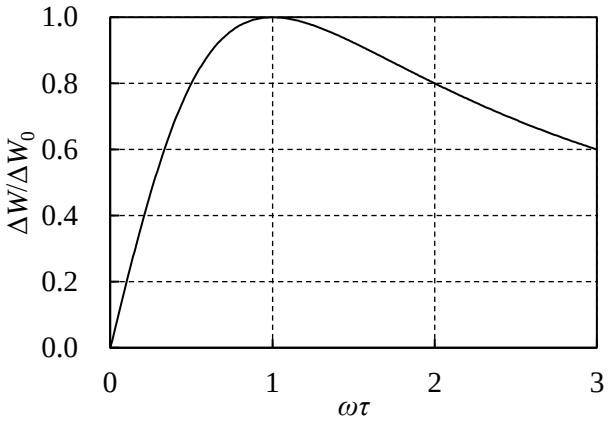

Fig. 8 Dissipated energy vs. frequency relationship

Meanwhile, if one end of a Maxwell material consisting of a spring with stiffness k and a dashpot with damping coefficient c connected in series is fixed, and the other end is moved at velocity v, the force F acting on the viscoelastic model follows Eq. (16).

$$\frac{1}{k}\frac{\mathrm{d}F}{\mathrm{d}t} + \frac{1}{c}F = v \tag{16}$$

As Eqs. (10) and (16) have the same form, their solutions also have the same form[21), 22)]. Therefore, if α_x in Eqs. (6) and (10) is considered constant, the damping force acting on the magnet can be expressed by a Maxwell element. Further, the coil behaves as an elastic body, and the resistor behaves as a viscous body.

3.1.2 For a copper plate

Consider the case in which eddy currents are generated in a nonmagnetic conductive plate (copper plate) near a vibrating magnet. The eddy current $\boldsymbol{i}$ is calculated from Eq. (17) using the current vector potential $\boldsymbol{T}$ that satisfies $\boldsymbol{i} = \mathrm{curl}\boldsymbol{T}$ [23)].

$$\mathrm{curl}\left(\frac{1}{\sigma}\mathrm{curl}\boldsymbol{T}(\boldsymbol{r})\right) + \mu_0\frac{\partial \boldsymbol{T}(\boldsymbol{r})}{\partial t} + \frac{\mu_0}{4\pi}\iint_S\left(\frac{\partial \boldsymbol{T}(\boldsymbol{r}')}{\partial t}\cdot\boldsymbol{n}\right)\frac{\boldsymbol{r}-\boldsymbol{r}'}{|\boldsymbol{r}-\boldsymbol{r}'|^3}\mathrm{d}S' = -\frac{\partial \boldsymbol{B}_m(\boldsymbol{r})}{\partial t} \tag{17}$$

where σ is the electrical conductivity (inverse of resistivity), $\boldsymbol{B}_m$ is the magnetic flux density due to the magnet, μ_0 is the permeability of a vacuum, $\boldsymbol{r}$ is the field point, $\boldsymbol{r}'$ is the source point, S is the surface of the copper plate, and $\boldsymbol{n}$ is the outward unit normal vector on the surface.

Comparing this equation with Eq. (10), the first term on the left-hand side corresponds to the resistor, the second and third terms correspond to the coil, and the right-hand side corresponds to the power

source. Furthermore, when using the thin-plate approximation[23], $\boldsymbol{T}$ only has a component T in the thickness direction, and Eq. (17) is scalarized. In this study, the conductor was discretized using the finite difference method, and a frequency response analysis was performed. Here, the integral of the third term on the left side was obtained analytically by bilinear interpolation of T between the nodes. Then, Eq. (17) was reduced to a simultaneous linear equation for T at all nodes. The obtained eddy current, $\boldsymbol{i} = \mathrm{curl}\boldsymbol{T}$, was used in Eq. (18) to calculate the damping force $\boldsymbol{F}$ acting on the magnet.

$$\boldsymbol{F} = -\iiint_V \boldsymbol{i}(\boldsymbol{r}) \times \boldsymbol{B}_m(\boldsymbol{r}) \mathrm{d}V \tag{18}$$

where V is the inside of the copper plate.

3.2 Evaluation of the damping characteristics of a copper plate

The damping characteristics of the magnetically levitated foundation with a copper plate shown in Fig. 2(b) were evaluated. As described in Section 2.2, the magnetically levitated foundation consisted of an aluminum body (200 mm × 200 mm × 65 mm) and four pairs of neodymium magnets (70 mm × 70 mm × 5 mm). A copper plate (200 mm × 200 mm × 5 mm) was placed above the magnets on the ground. The gap between the magnets was 21 mm. Section 3.1 shows that if the electrical resistance of the copper plate is reduced, the damping coefficient c increases when replaced with a viscoelastic model. In this study, we considered Case 1, in which the electrical conductivity of copper is equivalent to that at room temperature (60×10^6 S/m), and Case 2, in which the electrical conductivity is equivalent to that at liquid nitrogen temperature (600×10^6 S/m), based on the property that copper becomes more conductive at low temperatures[24]. In addition, we inserted a spacer under the copper plate in Case 2 and reduced the distance between the magnets at the bottom of the foundation and the copper plate from 16 mm to 8 mm, which is Case 3. Eddy currents were calculated using the method in Section 3.1.2. The magnets vibrated horizontally or vertically with a displacement amplitude of 1 mm. The vibration frequency was varied in the range of 1–10 Hz to include the natural frequency (approximately 6 Hz) of the test specimens used in Section 4.

Figure 9 shows the current density distribution in the copper plate in Case 2 when the magnet velocity is at its maximum with a vibration of 6 Hz. Here, the magnets move to the right of the paper in Fig. 9(a) and toward the front in Fig. 9(b). During the horizontal motion, current eddies in opposite directions exist between the left and right magnets, whereas during the vertical motion, the current circulates along the edge of the magnets. The reaction force of the force that these eddy currents receive from the magnetic field is the damping force.

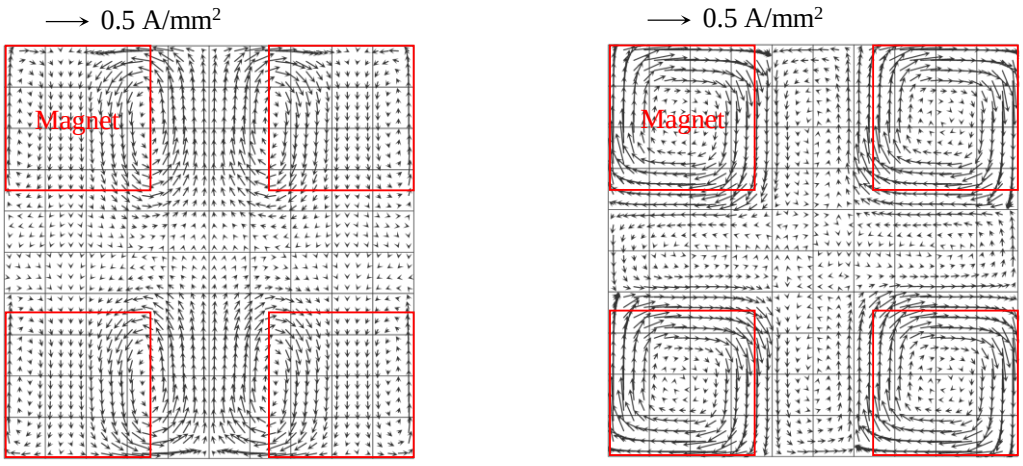

(a) During horizontal motion (b) During vertical motion

Fig. 9 Current density distribution in copper plate (Case 2)

Figure 10 shows the relationship between the energy ΔW dissipated by the damping force per cycle and the vibration frequency. This relationship is linear in Case 1, whereas in Cases 2 and 3, it follows a curve such that ΔW is maximum at 6 to 7 Hz because of self-induction. If the conductivity of the copper plate is increased beyond that in Cases 2 and 3, the energy is stored in the coil shown in Fig. 7(b) and is less likely to be consumed by the resistor, and the performance of the damper at approximately 6 Hz deteriorates.

The relationship between ΔW and frequency when the damping force in Case 1 is approximated by a dashpot and the damping force in Cases 2 and 3 is approximated by a Maxwell material is superimposed in Fig. 10. The fitted curves capture the tendency of the theoretical solution.

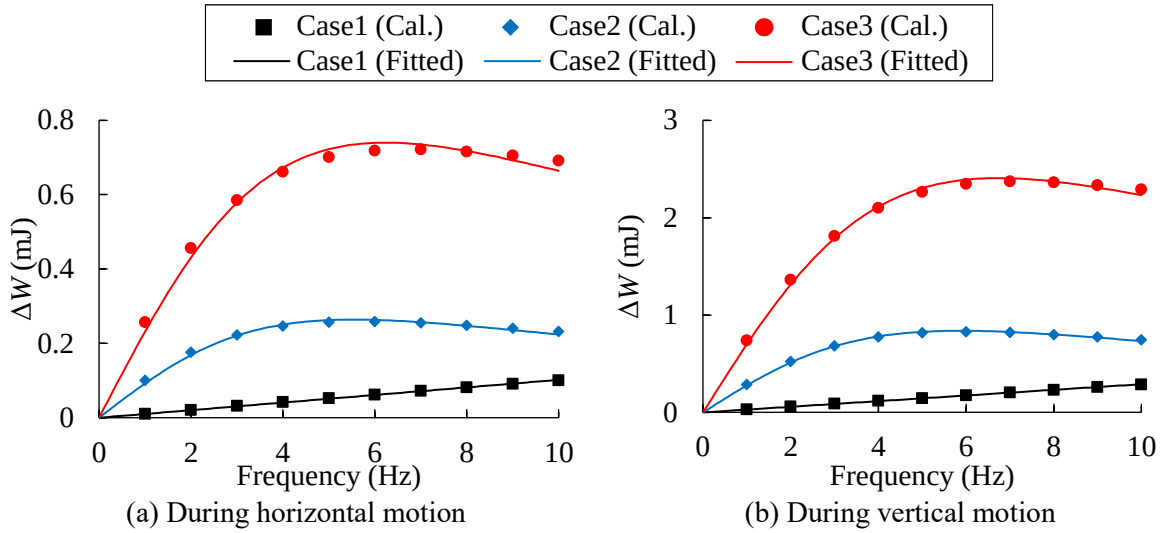

(a) During horizontal motion (b) During vertical motion

Fig. 10 Dissipated energy vs. frequency relationship

4. SHAKING TABLE EXPERIMENT AND 3D FEM ANALYSIS OF A BUILDING MODEL USING A MAGNETICALLY LEVITATED FOUNDATION

4.1 Specimens and conditions

In this section, the seismic response of a small-scale building model with a magnetically levitated foundation is examined through experiments and 3D finite element method (FEM) analysis. Figure 11 presents a list of the examined models. The examined models were those that used neither steel nor copper plates, those that used a steel plate, and those that used a copper plate. The responses of the models with magnets only and those with a steel plate were examined through both model shaking table experiments and simulation analysis, whereas the response of the model with a copper plate was examined based only on 3D FEM analysis. Because appropriate equipment is required to cool the copper plate safely with liquid nitrogen, the first objective is to understand the damping effect through analysis.

Photo 1 shows the test specimen. The model consisted of a building, displacement control material, and an acrylic container. The building consisted of a magnetically levitated foundation, steel columns, and a brass superstructure. The magnetically levitated foundation consisted of an aluminum body (200 mm × 200 mm × 65 mm) and four pairs of neodymium magnets (70 mm × 70 mm × 5 mm), as described in Sections 2.2 and 3.2. A 3.2 mm thick steel plate was used when the steel plate was installed, and a 5 mm thick copper plate was used when the copper plate was installed. The masses of the foundation, superstructure, and steel plate were 6.9, 6.7, and 0.99 kg, respectively, and the mass of each magnet was 0.18 kg. The mass ratio of the foundation to superstructure was approximately 1:1, assuming a two-story detached house. The natural frequency of the superstructure when the foundation was fixed was 9.5 Hz,

and the primary natural frequency of the coupled system of the displacement control material and the building when only magnets were installed was 6.1 Hz. The experimental values of the levitation height of the foundation (gap between magnets) were approximately 21 mm when only magnets were installed and approximately 25 mm when the steel plate was installed. The mass and levitation height of the foundation with the copper plate were assumed to be the same as those of the foundation with magnets only.

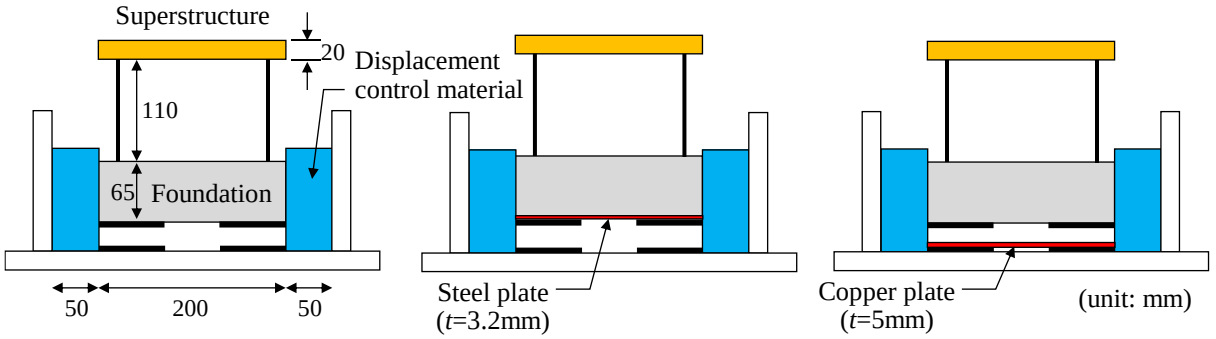

(a) Magnet only (Test & analysis) (b) With steel plate (Test & analysis) (c) With copper plate (Analysis only)

Fig. 11 Building models using magnetically levitated foundation

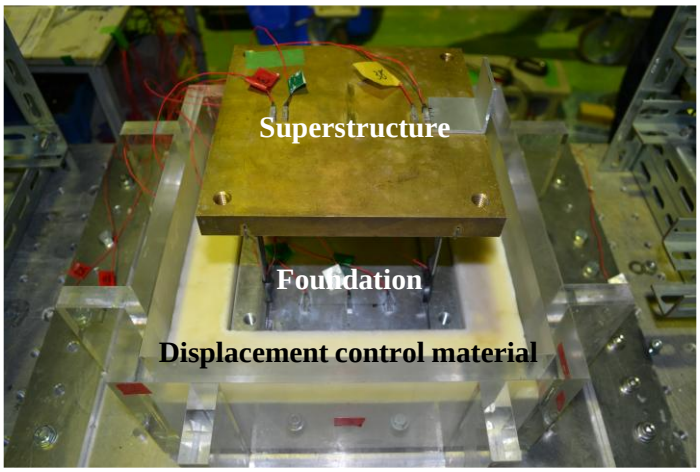

Photo 1 Appearance of the test specimen

Magnesium acrylate polymer was used as a displacement control material to support the sides of the foundation. This material is fabricated by polymerizing magnesium acrylate (monomer), and the curing period required for polymerization is approximately 3 days. Figure 12 shows the stress–strain relationship of the displacement control material in the uniaxial compression test. This material has high linearity, even for large strains exceeding 10%. In Ref. 9), the high damping properties of the magnesium acrylate polymer were confirmed by cyclic simple shear tests, although in the condition in which sand was mixed.

The input earthquake motion was a waveform adapted to the acceleration response spectrum specified at the ground surface of Type 2 ground using a simplified method of limit strength calculation in the Japanese design code. The JMA Kobe NS phase of the 1995 Hyogo-ken Nanbu earthquake was used. Because a small model with a high natural frequency was utilized in this experiment, the time axis of the time history was reduced to one-tenth of its original size, considering the law of similarity, and the amplitudes were changed to 0.2, 0.5, 1.0, and 1.5 times the input.

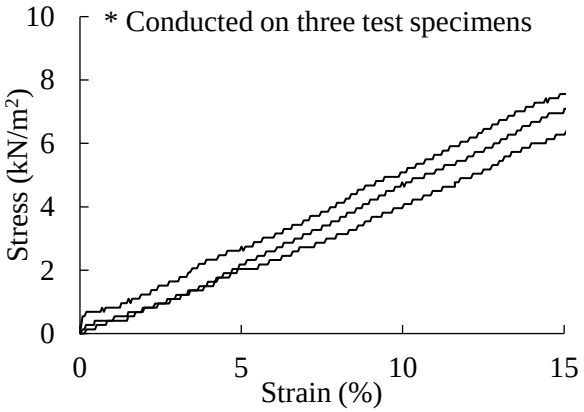

Fig. 12 Uniaxial compression test results for displacement control material

4.2 Conditions for 3D FEM analysis

The response at 0.2 times input was the subject of analysis. LS-DYNA was used.

The analytical model is illustrated in Fig. 13. The foundation and steel plate were modeled using rigid solid elements. The horizontal and rotational movements of the foundation were considered, but the vertical movement of the center of gravity was not. The superstructure was modeled as a linear lumped mass system. In this case, to consider the horizontal displacement owing to the rocking of the foundation, the superstructure was represented by a double node located at its center, where one node was subordinate to the foundation and moved as a rigid body together with it, and a mass of 6.7 kg was concentrated at the other node. The two nodes were connected with a spring and dashpot that simulated columns. A horizontal stiffness of 24.6 N/mm was estimated with reference to the vibration results when the foundation was fixed, and viscous damping with a damping constant of approximately 0.5% was provided. The displacement control material was modeled using elastic solid elements. The Young's modulus of the displacement control material was set to 0.0488 N/mm^2 based on the results of a uniaxial compression test, and Poisson's ratio was set to 0.4997. Furthermore, the displacement-control material, which is a polymer, is believed to exhibit viscoelasticity. In this study, it was assumed for simplicity that the displacement control material can be represented by a Voigt material, and stiffness-proportional damping was applied to represent the viscous term. The damping constant at the first natural frequency of the coupled system was set to 8% so that the response of the top of the superstructure at 0.2 times the input matched the experimental results. The contact surfaces of the displacement control material, foundation, and container were in tight contact, whereas those of the container were rigid.

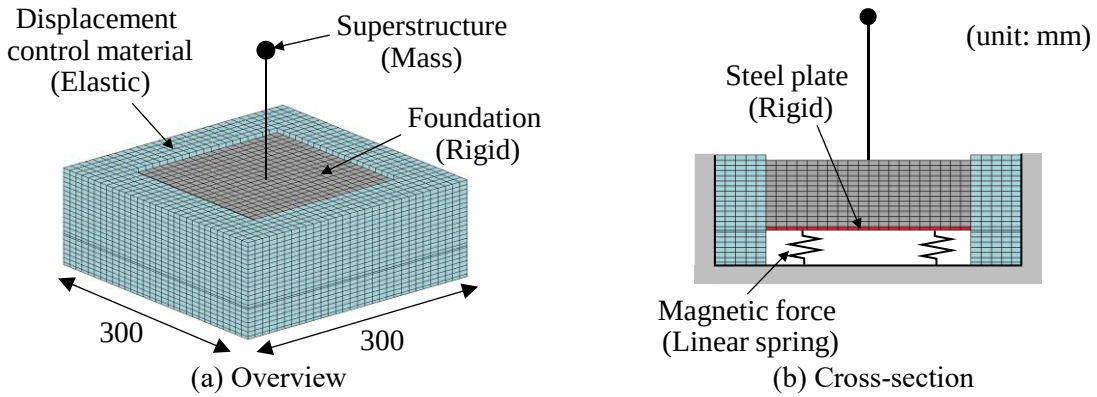

Fig. 13 3D FEM model of magnetically levitated building model (with steel plate)

The vertical, horizontal, and rotational resistances of the foundation caused by the magnetic force acting on the magnet and steel plate were modeled using linear spring elements based on the theoretical

solution obtained in Section 2.2. Here, the relationship between the magnetic force and displacement was nonlinear, as shown in Fig. 4. However, because the displacement of the foundation was small in this experiment, the tangential stiffness at the position where the foundation displacement was zero was used.

The damping force due to eddy currents in the model with the copper plate was modeled with a dashpot in Case 1 and with a Maxwell element in Cases 2 and 3, based on the analysis results in Section 3.2. A small mass was assigned to the intermediate nodes of the viscoelastic model in Cases 2 and 3 to stabilize the calculations.

4.3 Effect of magnetic material on the response of building model

Figure 14 shows the Fourier amplitude ratio of the superstructure response to the input. The Fourier amplitude was smoothed using a Parzen window with a bandwidth of 0.5 Hz. Compared with the fixed foundation model, the dominant frequency of the response of the magnetically levitated foundation model was lower, and the peak value was smaller. The decrease in the dominant frequency was attributed to the deformation of the displacement control material, which allowed the foundation to move in a swaying and rocking manner. At 1.5 times the input, the dominant frequency was even lower, and the amplification factor was smaller. The nonlinearity of the specimen response was experimentally confirmed in Ref. 7), indicating the effect of separation at the contact surface between the foundation and displacement control material[7]. In addition, when comparing the presence and absence of a steel plate, the Fourier amplitude ratio at 1.5 times the input was almost the same, whereas at 0.2 times the input, the dominant frequency was lower in the model with the steel plate.

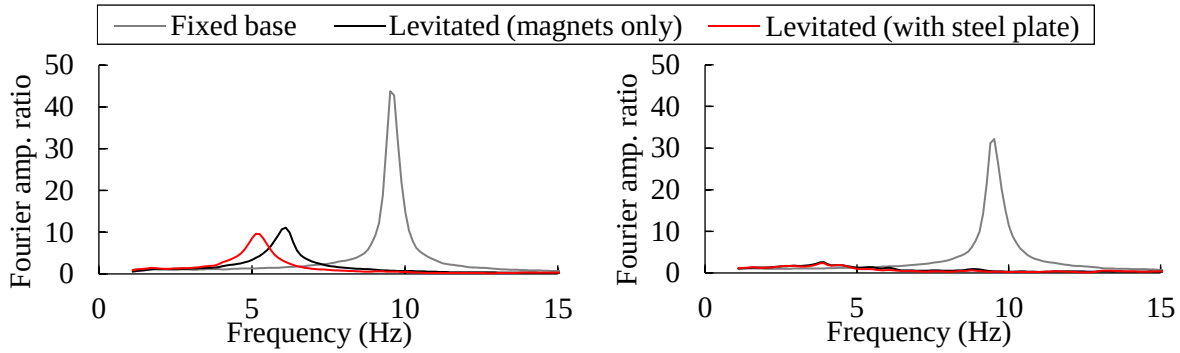

Fig. 14 Fourier acceleration amplitude ratio of superstructure response to input

Figure 15 shows the Fourier amplitude ratio of the superstructure response to the input obtained in the analysis of the 0.2 times input, compared with the experimental results. The analysis results for the model only with magnets correspond to the experimental results for both the dominant frequency and peak value. However, a difference in the superstructure response due to the presence or absence of the steel plate does not appear in the analysis results. In this analysis, the differences in the mass of the foundation and the stiffness of the magnetic spring were considered. However, the mass of the steel plate was only approximately 1/7 the mass of the aluminum part of the foundation. Although the magnetic force acting on the foundation increases owing to the magnetization of the steel plate, if the gap between the magnets is the same, the foundation levitates more; thus, the result is approximately the same as that when there is no steel plate. Therefore, it can be concluded that the effects of these factors on the superstructure response were small. Another factor is that in the model with the steel plate, separation of the contact surface between the foundation and displacement control material occurred early, which reduced the resistance of the displacement control material to the swaying and rocking motions of the foundation.

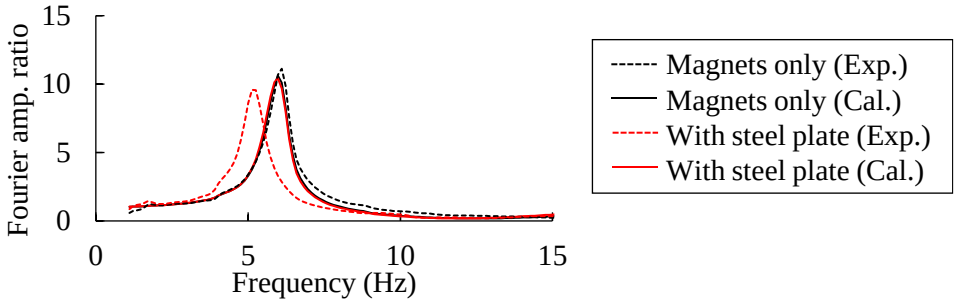

Fig. 15 Comparison of experiment and analysis

4.4 Effects of eddy currents on the response of building models

Figure 16(a) shows the acceleration time history waveform of the superstructure response as an analysis result for the model using a copper plate. In Case 3, the maximum acceleration was approximately the same as that in the magnet-only test specimen; however, the response decayed quickly after 1.5 s when the input became small. Figure 16(b) shows the Fourier amplitude ratio of the superstructure response to the input. The peak value of the amplitude ratio decreased in Case 3, which corresponded to an increase in the damping of the displacement control material by approximately 20%. Note that, in this experiment, as in the experiment in Ref. 8), although the stiffness of the displacement control material was made as low as possible, the contribution of the displacement control material to the foundation impedance is dominant. However, it is believed that the effect of the eddy current damper is more pronounced when the damping of the displacement control material is small.

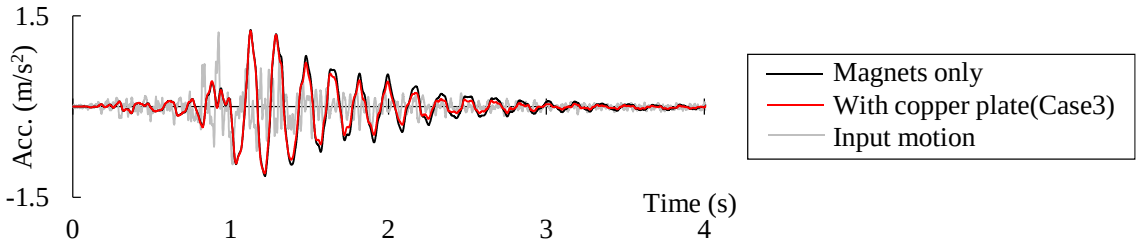

(a) Acceleration time history

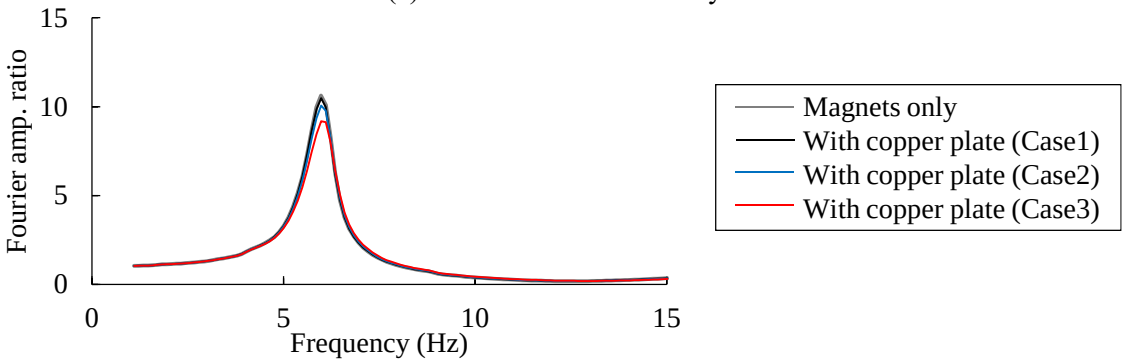

(b) Fourier acceleration amplitude ratio of superstructure response to input

Fig. 16 Earthquake response of the upper mass point of the model with the copper plate inserted

5. CONCLUSIONS

To reduce the earthquake response of buildings, the authors propose a magnetically levitated foundation with a displacement control material supporting the foundation side and permanent magnets insulating the bottom surface of the foundation. In this study, the levitation force and damping of a foundation

were improved by magnetizing a steel plate and generating eddy currents on a copper plate. The findings are as follows:

[1] When a steel plate is placed above the magnets at the bottom of the foundation, the levitation force of the foundation increases owing to the repulsion between the magnetized steel plate and the magnet on the ground. This was confirmed by static load tests and the static magnetic field theory.

[2] The properties of the eddy currents generated by the copper plate between the magnets and the resulting damping force were examined from the theory of electromagnetic induction. Focusing on the form of the equation satisfied by the eddy currents, it was shown that the damping force can be expressed by a Maxwell material. In particular, the elastic behavior corresponds to self-induction, in which eddy currents hinder their own changes, and the energy consumption does not increase without limit even if the electrical resistance of the copper plate is reduced or the vibration frequency is increased.

[3] The vibration characteristics of building models in which the displacement control material, magnetically levitated foundation, and superstructure were coupled were examined. First, the shaking table experiments confirmed that when a steel plate was used, the foundation levitated more, whereas mechanical stability was maintained through support from the displacement control material. The FEM analysis also demonstrated that a certain degree of damping could be imparted to the structure by using a copper plate with low electrical resistance. This shows that the levitation force and damping of the foundation can be improved by utilizing the magnetization and eddy currents in the insulating layer, respectively, although the electromagnetic phenomenon becomes more complex. A future challenge is to achieve low-temperature conditions to lower the electrical resistance of the copper plates.

ACKNOWLEDGMENT

We received cooperation from Tomotaka MATSUI of Toagosei Co., Ltd. for the creation of the test specimens for this experiment. For this research, we also received cooperation from the University of Osaka graduates Kentaro SHO and Yuki OHATA, and the University of Osaka graduate students Hiaki NISHIMURA and Miharu OHTANI. We express our gratitude to them.

REFERENCES

1) Mizuno, T., Yano, K., Kanemitsu, Y. and Watanabe, K.: Research on Electromagnetically-Levitated Vibration Isolation System, (Part 1) Outline of Two-Dimensional Vibration Isolation System and Control Method, *Summaries of Technical Papers of Annual Meeting*, *Architectural Institute of Japan*, *Structure I*, pp. 621–622, 1993 (in Japanese).
2) Tsuda, M., Kojima, T., Yagai, T. and Hamajima, T.: Vibration Characteristics in Magnetic Levitation Type Seismic Isolation Device Composed of Multiple HTS Bulks and Permanent Magnets, *IEEE Transactions on Applied Superconductivity*, Vol. 17, No. 2, pp. 2059–2062, 2007.
3) Kurosawa, E., Kuramoto S., Saruki, Y., Nakamura K. and Miyazaki, T: Person of MECHALIFE, No.25, Air Determination Tremble Developer [Tsu-baihaujingu] Ltd. Representative Shoichi SAKAMOTO, *Journal of the Society of Mechanical Engineers*, Vol. 113, No. 1099, pp. 451–455, 2010 (in Japanese).
4) Yasuda, M., Sato, E., Yamada, M., Kajiwara, K. and Hayatsu, M.: Development of Three-Dimensional Seismic Isolation System Using Negative Stiffness Link Mechanism and Air Levitation Mechanism in Series (Overview of Prototype Experimental Device and Report on Full-Scale 3-D Seismic Excitation Experiment by E-Defense Shaking Table), *Transactions of the JSME*, Vol. 83, No. 851, 17-00057, 2017 (in Japanese).
5) Earnshaw, S.: On the Nature of the Molecular Forces which Regulate the Constitution of the Luminiferous Ether, *Transactions of the Cambridge Philosophical Society*, Vol. 7, pp. 97–112, 1842.
6) Miyamoto, Y., Shimamura, A., Fujii, S., Hoshizawa, F. and Kashiwa, H.: A Fundamental Study on the Earthquake Response Reduction of Base-Isolated Foundation Backfilled Using an Improved Compound Geomaterial, *Japan Architectural Review*, Vol. 1, No. 1, pp. 56–66, 2018.

7) Miyamoto, Y., Nakano, T., Shimamura, A. and Sho, K.: Seismic Response of Magnetically Levitated House, *Open Journal of Earthquake Research*, Vol. 11, No. 1, pp. 1–17, 2022.
8) Nakano, T., Miyamoto, Y. and Kashiwa, H.: Shaking Table Test and Analysis on Base-Insulated Building Model Using Displacement Control Material and Permanent Magnet, *Journal of Structural Engineering*, Vol. 70B, pp. 185–193, 2024 (in Japanese).
9) Shimamura, A., Umakoshi, M., Miyamoto, Y., Igarashi, D. and Goto, A.: Development of Compound Geo-Material with Magnesium Acrylate and Experimental Study on the Earthquake Response Reduction, (Part 1), *Summaries of Technical Papers of Annual Meeting*, *Architectural Institute of Japan*, *Structure II*, pp. 821–822, 2016 (in Japanese).
10) Kato, M.: *Electromagnetism*, The University of Tokyo Press, Tokyo, Japan, pp. 147–149, 1987 (in Japanese, title translated by the authors).
11) Miya, K.: *Analytical Electromagnetism and Electromagnetic Structures*, Yokendo, Tokyo, Japan, pp. 94–101, 1995 (in Japanese, title translated by the authors).
12) Ohta, K.: *Fundamentals of Electromagnetism I*, The University of Tokyo Press, Tokyo, Japan, pp. 239–241, 2012 (in Japanese, title translated by the authors).
13) Sunagawa, S.: *Theoretical Electromagnetism*, 3rd ed., Kinokuniya Company, Tokyo, Japan, pp. 22–27, 1999 (in Japanese, title translated by the authors).
14) Sato, T. and Inui, Y.: Three Dimensional Static Magnetic Field Calculation by Equivalent Current of Magnetization Vector and Its Applications, *The Transactions of the Institute of Electrical Engineers of Japan B*, Vol. 100, No. 3, pp. 177–183, 1980 (in Japanese).
15) Yamazaki, K., Ogawa, T., Kushibe, A., Ishihara, D., Nakano, M., Fujiwara, K., Takahashi, N. and Chiba, A.: Estimation of the Deterioration of Structural Materials on the Basis of Changes in Their Magnetization Properties during the Application of Tensile Stress, *Journal of the Magnetics Society of Japan*, Vol. 23, No. 4-2, pp. 1541–1544, 1999 (in Japanese).
16) Teshima, Y., Gotoh, Y. and Takahashi, N.: Non-Destructive Slack Inspection Technique for High Tension Bolts Using the Electromagnetic Phenomenon, *Journal of The Japanese Society for Non-Destructive Inspection*, Vol. 61, No. 5, pp. 227–234, 2012 (in Japanese).
17) Shi, Z., Loong, C. N. and Shan, J.: Equivalent Circuit Model of Eddy Current Damping Regarding Frequency Dependence with Test Validation, *Advances in Structural Engineering*, Vol. 25, No. 1, pp. 188–200, 2022.
18) Yamane, K., Takayama, Y., Kijimoto, S. and Ishikawa, S.: Modeling of Magnetic Damper Composed of Ring Magnet and Coaxially and Relatively Moving Conducting Disk Considering Skin Effect, *Transactions of the JSME*, Vol. 82, No. 837, 15-00659, 2016 (in Japanese).
19) Sunagawa, S.: *Theoretical Electromagnetism*, 3rd ed., Kinokuniya Company, Tokyo, Japan, pp. 168–172, 1999 (in Japanese, title translated by the authors).
20) Ohta, K.: *Fundamentals of Electromagnetism I*, The University of Tokyo Press, Tokyo, Japan, pp. 192–193, 2012 (in Japanese, title translated by the authors).
21) Feynman, R. P., Leighton, R. B. and Sands, M.: *The Feynman Lectures on Physics*, *Volume II*, *Mainly Electromagnetism and Matter*, Addison-Wesley, Boston, USA, pp. 12-1–12-13, 1964.
22) Nagamatsu, M. and Nagamatsu, A.: Development and Application of Unified Model of Electric and Mechanical System, 2nd Report, Introduction of New Analogy between Mechanics and Electromagnetics, *Journal of the Japan Society for Simulation Technology*, Vol. 32, No. 2, pp. 136–143, 2013 (in Japanese).
23) Miya, K.: *Analytical Electromagnetism and Electromagnetic Structures*, Yokendo, Tokyo, Japan, pp. 187–202, 1995 (in Japanese, title translated by the authors).
24) Sasaki, W.: Electrical Conduction at Cryogenic Temperatures, *The Journal of the Institute of Electrical Engineers of Japan*, Vol. 78, No. 834, pp. 84–90, 1958 (in Japanese, title translated by the authors).

(Original Japanese Paper Published: January, 2025)
(English Version Submitted: February 12, 2025)
(English Version Accepted: February 25, 2025)